Journal of Hazardous Materials 178 (2010) 42–48

Contents lists available at ScienceDirect

Journal of Hazardous Materials

journal homepage: www.elsevier.com/locate/jhazmat

Prediction of uranium and technetium sorption during titration of contaminated acidic groundwater

Fan Zhang[a,*], Jack C. Parker[b], Scott C. Brooks[c], David B. Watson[c], Philip M. Jardine[d], Baohua Gu[c]

[a] Institute of Tibetan Plateau Research, Chinese Academy of Sciences, 18 Shuangqing Road, P.O. Box 2871, Beijing 100085, China
[b] Department of Civil and Environmental Engineering, University of Tennessee, Knoxville, TN 37996, USA
[c] Environmental Sciences Division, Oak Ridge National Laboratory, Oak Ridge, TN 37831-6038, USA
[d] Biosystems Engineering and Soil Science Department, University of Tennessee, Knoxville, TN 37996, USA

ARTICLE INFO

Article history:
Received 20 October 2009
Received in revised form 8 January 2010
Accepted 8 January 2010
Available online 15 January 2010

Keywords:
Radionuclide
Sulfate
Aluminum
pH
Anion exchange
Model

ABSTRACT

This study investigates uranium and technetium sorption onto aluminum and iron hydroxides during titration of acidic groundwater. The contaminated groundwater exhibits oxic conditions with high concentrations of NO_3^-, SO_4^{2-}, U, Tc, and various metal cations. More than 90% of U and Tc was removed from the aqueous phase as Al and Fe precipitated above pH 5.5, but was partially resolublized at higher pH values. An equilibrium hydrolysis and precipitation reaction model adequately described variations in aqueous concentrations of metal cations. An anion exchange reaction model was incorporated to simulate sulfate, U and Tc sorption onto variably charged (pH-dependent) Al and Fe hydroxides. Modeling results indicate that competitive sorption/desorption on mixed mineral phases needs to be considered to adequately predict U and Tc mobility. The model could be useful for future studies of the speciation of U, Tc and co-existing ions during pre- and post-groundwater treatment practices.

1. Introduction

Remediation of sites containing highly radioactive wastes that pose risks to human health and the environment is one of the largest environmental problems facing the U.S. Department of Energy (DOE) [1]. Uranium (U) and technetium (Tc) are prevalent radionuclide contaminants throughout the DOE weapons complex. Uranium is the most frequently detected and Tc is the eighth most frequently detected radionuclide in contaminated groundwater and sediments [2]. Tc (as pertechnetate, TcO_4^- anion) is not particularly reactive with soil minerals, and exhibits greater mobility than U, which is more reactive with soil and sediment minerals [3]. The remediation of radionuclides U and Tc in groundwater largely depends on biogeochemical conditions, such as pH, redox potential, microbial community, the availability of suitable electron donors, and the presence or absence of various metals. High metal and nitrate concentrations and low pH conditions at waste sites pose formidable challenges to successful implementation of in situ bioimmobilization. Aquifer pH exerts strong effects on precipitation, redox, complexation and sorption reactions and hence on contaminant mobility [4]. The ability to predict acid–base behavior of the groundwater is critical to predict U and Tc transport under variable pH conditions.

Uranium exhibits two primary oxidation states in groundwater—U(VI) and U(IV) [5]. The U(VI) uranyl ion (UO_2^{2+}) is most stable under acidic or oxygenated conditions [6]. Technetium exhibits two primary oxidation states in groundwater—Tc(VII) and Tc(IV) [7]. The Tc(VII) pertechnetate ion (TcO_4^-) is most stable under oxidizing conditions [8]. Therefore, under oxic conditions, uranium and technetium are anticipated to be present in groundwater as the uranyl (UO_2^{2+}) and pertechnetate (TcO_4^-) ions [9]. However, U(VI) speciation is also complicated by formation of negatively-charged strong carbonate complexes $UO_2(CO_3)_2^{2-}$ and $UO_2(CO_3)_3^{4-}$ under neutral or alkaline pH conditions [5]. Unlike UO_2^{2+}, pertechnetate anions do not form carbonate species [10].

Previous studies have shown that Fe and Al minerals sorb/coprecipitate with dissolved sulfate [11], U [12,13] and Tc [14,15] species. At pH < 5, sorption of TcO_4^- on hematite has been explained in terms of electrostatic attractions between positively charged hematite colloids and the pertechetate anions [14]. Sorption of TcO_4^- on Mg/Al layered hydroxides was found to be a stepwise ion exchange process [15]. Sorption of U(VI) onto Fe hydroxides has been extensively modeled [16,17]. However, reliable thermodynamic data are not available to simulate sorption of U(VI) by Al hydroxides, or sorption of Tc by Fe or Al hydroxides.

In the present study, we newly develop an ion exchange reaction model for the sorption of uranium and technetium onto Al and Fe hydroxides in competition with sulfate to predict dissolved radionuclide concentrations at pre/post-titration conditions needed to design successful immobilization and bioremediation

* Corresponding author. Tel.: +86 10 62849383; fax: +86 10 62849886.
E-mail address: zhangfan@itpcas.ac.cn (F. Zhang).

0304-3894/$ – see front matter © 2010 Elsevier B.V. All rights reserved.
doi:10.1016/j.jhazmat.2010.01.040

strategies. To simulate dynamic pH-dependent anion exchange capacity, Al and Fe hydroxides were treated as a polyprotic base controlled by mineral precipitation and dissolution reactions to simulate changes in solid phase surface site density. The complex behavior of multiple competing anions with a wide range of concentrations in the contaminated groundwater is investigated considering various aqueous phase and precipitation/dissolution reactions occurring over a wide range in pH. Electrostatics favor SO_4^{2-}, $UO_2(CO_3)_2^{2-}$, and $UO_2(CO_3)_3^{4-}$ sorption over TcO_4^- in ion exchange reactions. However, this investigation reveals extremely high affinity for TcO_4^- sorption on Al and Fe hydroxides, which is perhaps supported by the fact that TcO_4^- is a large, poorly hydrated anion and has a natural tendency to be strongly sorbed by a variety of adsorbents [8,10,18].

2. Experimental and computational methods

2.1. Groundwater and characterization

The groundwater samples used for the titration experiment were obtained from monitoring well FW-026 at the Oak Ridge Field Research Center at the Y-12 National Security Plant site in Oak Ridge, Tennessee. The acidic groundwater (pH ~ 3.8) contains high concentrations of radionuclides U (~0.212 mM) and Tc (~16.1 nM), metal ions including Ni (~0.212 mM) and Co (~39.7 μM), Al (~16.8 mM), Ca (~23.4 mM), Mg (~6.56 mM), Mn (~2.35 mM) and Fe (~0.243 mM), and anions such as NO_3^- (~123 mM) and SO_4^{2-} (~10.2 mM) [4]. The groundwater is also characterized with a high dissolved oxygen (DO) content at 2–4 mg L^{-1}, in which uranium exists primarily as uranyl or U(VI) species in water [4,19,20]. It was therefore kept refrigerated under aerobic conditions until used.

2.2. Titration experiments

Titration of contaminated groundwater was performed in batch experiments to evaluate precipitation and/or dissolution/desorption of contaminant metals and radionuclides under varying pH conditions. Because of the production of carbonate or bicarbonate species during microbial respiration, both NaOH and Na_2CO_3 were used for titration to study their effects on precipitation and/or coprecipitation of metal/radionuclide contaminants. The contaminated groundwater (20 mL) was placed in a series of polyethylene vials, to which various amounts (0–1.2 mL) of either 2 M NaOH or Na_2CO_3 were added to give a pH range between 3.8 and 9. All samples were prepared under ambient conditions and the final volume was made up to 21.2 mL. The sample vials were placed on an end-over-end shaker for 2 days before the final pH measurement. The suspension was filtered with a 0.2 μm polytetrafluoroethylene syringe filter and the clear supernatant solution was analyzed for dissolved elements (e.g., Al, Fe, Ca, Mg, Mn, Co, Ni, K, and Si) by inductively coupled plasma, common anions (e.g., SO_4^{2-}, NO_3^- ,and Cl^-) by ion chromatography, U by steady state phosphorescence, and Tc by liquid scintillation counting. Based on duplicate analyses of selected samples, analytical errors were estimated to be about 10%, considering possible interferences and dilutions necessary for the analysis of groundwater constituents over the observed concentration range. Precipitated solids from selected samples were analyzed for mineralogical characteristics. It should be pointed out that CO_2 was not excluded in the NaOH experimental system, although the system might not be equilibrated with the atmosphere because of a limited headspace.

2.3. Modeling tools

The computer code HydroGeoChem v5.0 (HGC5) [21], a comprehensive model for fluid flow, thermal and reactive transport, was used to analyze experimental results. The program is designed for generic biogeochemical reaction networks, which may include both equilibrium and kinetic reactions with user specified formulations [22]. The biogeochemical reactive transport module of HGC5 was run in batch mode to calculate equilibrium distributions of elements between aqueous and solid phases. Iterative calculations were performed to identify controlling precipitation and dissolution reactions and to solve for individual species concentrations [4]. The Gaines–Thomas [23] selectivity coefficient formulation was used for ion exchange reactions. HGC5 was coupled with the nonlinear inversion code PEST [24] to enable calibration of specified model coefficients from measured data. The regression analyses were carried out using the whole set of reactions to calibrate the measured sulfate, U and Tc concentrations. Logarithms of concentrations were employed to give equal relative weight to all data points [25].

2.4. Reaction path model

The geochemical processes governing changes in solution composition during titration were simulated using two reaction models. Both models assumed the titration system to be closed to the atmosphere, i.e., we did not assume equilibrium with atmospheric CO_2 [20]. For the NaOH titration, the titrant was assumed to contain 0.07 mol of total carbonate per mole NaOH [4,20]. The aqueous concentration of Fe(II) was assumed to be negligible because of a low total Fe concentration in the aquifer material and a relatively high dissolved oxygen concentration in groundwater [20]. In the investigated groundwater system, dissolved Fe concentrations are low relative to Al. However, because other areas of the study site have high Fe levels which are expected to play an important role in sorption of uranium [16], Fe is included in the model in this study.

Table 1
Solid phases considered in the reaction models.

Reactions	log *K*
$Al(OH)_{3(s)}$ (microcrystalline gibbsite) + $3H^+ = Al^{3+} + 3H_2O$	9.35[a]
$Al_4SO_4(OH)_{10}\cdot 5H_2O_{(s)}$ (basaluminite) + $10H^+ = 4Al^{3+} + SO_4^{2-} + 15H_2O$	25.0[b]
$SiO_{2(s)}$ (amorphous silica) + $2H_2O = Si(OH)_4^0$	−2.71[a]
$Al_2Si_2O_5(OH)_{4(s)}$ (kaolinite) + $6H^+ = 2Al^{3+} + 2Si(OH)_4^0 + H_2O$	7.435[a]
$Ca(OH)_{2(s)}$ (portlandite) + $2H^+ = Ca^{2+} + 2H_2O$	22.8[a]
$CaCO_3\cdot H_2O_{(s)}$ (monohydrocalcite) = $Ca^{2+} + CO_3^{2-} + H_2O$	−7.60[b]
$CaSO_4\cdot 2H_2O_{(s)}$ (gypsum) = $Ca^{2+} + SO_4^{2-} + 2H_2O$	−4.58[a]
$Mg(OH)_{2(s)}$ (brucite) + $2H^+ = Mg^{2+} + 2H_2O$	16.84[a]
$MgCO_{3(s)}$ (magnesite) = $Mg^{2+} + CO_3^{2-}$	−7.5[a]
$CaMg(CO_3)_{2(s)}$ (disordered dolomite) = $Ca^{2+} + Mg^{2+} + 2CO_3^{2-}$	−16.54[b]
$Mn(OH)_{2(s)}$ (pyrolusite) + $2H^+ = Mn^{2+} + 2H_2O$	15.2[a]
$MnCO_{3(s)}$ (synthetic rhodocrosite) = $Mn^{2+} + CO_3^{2-}$	−10.39[b]
$Ni(OH)_{2(s)}$ (theophrastite) + $2H^+ = Ni^{2+} + 2H_2O$	10.8[b]
$NiCO_{3(s)} + H^+ = Ni^{2+} + HCO_3^-$	3.512[b]
$UO_2CO_{3(s)}$ (rutherfordine) + $H^+ = UO_2^{2+} + HCO_3^-$	−4.143[b]
$UO_3\cdot 2H_2O_{(s)}$ (schoepite) + $2H^+ = UO_2^{2+} + 3H_2O$	4.812[b]
$(UO_2)_2SiO_4\cdot 2H_2O_{(s)}$ (soddyite) + $4H^+ = 2UO_2^{2+} + Si(OH)_4^0 + 2H_2O$	5.74[b]
$Na_2(UO_2)_2(Si_2O_5)_3\cdot 5H_2O_{(s)}$ (Na-weeksite) + $6H^+ + 5H_2O = 2Na^+ + 2UO_2^{2+} + 6Si(OH)_4^0$	1.51[b]
$Co(OH)_{2(s)} + 2H^+ = Co^{2+} + 2H_2O$	12.1[b]
$CoCO_{3(s)}$ (sphaerocobaltite) + $H^+ = Co^{2+} + HCO_3^-$	−0.233[b]
$SrCO_{3(s)}$ (strontianite) = $Sr^{2+} + CO_3^{2-}$	−9.271[a]
$SrSO_{4(s)}$ (celestite) = $Sr^{2+} + SO_4^{2-}$	−6.63[a]
$FeCo_{0.1}(OH)_{3.2(s)} + 3.2H^+ = Fe^{3+} + 0.1Co^{2+} + 3.2H_2O$	5.7[b]
$UO_2SO_4\cdot 2.5H_2O_{(s)} = UO_2^{2+} + SO_4^{2-} + 2.5H_2O$	−1.589[c]
$UO_2SO_4\cdot 3H_2O_{(s)} = UO_2^{2+} + SO_4^{2-} + 3H_2O$	0.831[c]
$UO_2SO_4\cdot 3.5H_2O_{(s)} = UO_2^{2+} + SO_4^{2-} + 3.5H_2O$	−1.585[c]

[a] Ref. [26].
[b] Ref. [20].
[c] Ref. [27].

Table 2
Ion exchange reactions developed in the model.

Reaction	Reaction parameter	Estimate ± Std dev.
$f\,\Sigma$ (Al&Fe precipitates) = $Y(OH)_2 + YOH^+ + Y^{2+}$	f[a]	0.331 ± 0.038
$YOH^+ + H_2O = Y(OH)_2 + H^+$ [b]	$\log K_{Y1}$	−8.78 ± 0.35
$Y^{2+} + H_2O = YOH^+ + H^+$	$\log K_{Y2}$	−4.91 ± 0.60
$A_2SO_4 + UO_2(CO_3)_2^{2-} = A_2UO_2(CO_3)_2 + SO_4^{2-}$ [c]	$\log K_{U1}$	1.81 ± 0.13
$2A_2SO_4 + UO_2(CO_3)_3^{4-} = A_4UO_2(CO_3)_3 + 2SO_4^{2-}$ [c]	$\log K_{U2}$	−0.574 ± 0.298
$2ATcO_4 + SO_4^{2-} = A_2SO_4 + 2TcO_4^-$ [c]	$\log K_{Tc}$	−3.68 ± 0.21

[a] f is the fraction of Al and Fe precipitates assumed to produce surfaces with neutral or positive charge.
[b] $Y(OH)_2$ is the hypothetical polyprotic base.
[c] A_2SO_4, $A_2UO_2(CO_3)_2$, $A_4UO_2(CO_3)_3$ and $ATcO_4$ are ion exchanged species of aqueous SO_4^{2-}, $UO_2(CO_3)_2^{2-}$, $UO_2(CO_3)_3^{4-}$ and TcO_4^-, respectively.

Model M1 considers aqueous complexation reactions of carbonate, sulfate, nitrate, chloride, K, Ca, Mg, Mn, Fe, Al, Si [26] and U [27] (details are provided in Table A.1), and precipitation/dissolution reactions (Table 1). X-ray diffraction analysis indicated that the precipitated solids were dominated by amorphous or poorly crystalline materials. Therefore, the solid phases shown in Table 1 were considered.

Model M2 considers additional anion exchange reactions of sulfate, U and Tc onto positively charged surfaces of Al and Fe hydroxide precipitates. Studies have shown that the ability of soils to adsorb SO_4^{2-}, U, and Tc are strongly influenced by pH and the amount of Al and Fe oxyhydroxides [11–15,28,29]. Speciation results for the M1 model indicated that the dominant species of aqueous uranium changes from $UO_2^{2+} \rightarrow UO_2CO_3^0 \rightarrow UO_2(CO_3)_2^{2-} \rightarrow UO_2(CO_3)_3^{4-}$ as pH increases from ~3.8 to above 8 in groundwater titrated with NaOH or Na_2CO_3. Therefore, in addition to precipitation, sorption of negatively-charged SO_4^{2-}, $UO_2(CO_3)_2^{2-}$, $UO_2(CO_3)_3^{4-}$,and TcO_4^- onto variably charged Al and Fe hydroxide surfaces was also considered as a mechanism exerting control on dissolved concentrations of anions in solution, simulated by anion exchange reactions (Table 2). A fraction (f) of Al and Fe precipitates generated during titration were assumed to produce surfaces with neutral or positive charge (Table 2). pH-dependent anion exchange capacity (AEC) associated with the solids was represented by ionization of a hypothetical polyprotic base $Y(OH)_2$ (Table 2) computed as $AEC = YOH^+ + 2Y^{2+}$. The reaction parameters of the ion exchange reactions (Table 2) were calibrated using the nonlinear parameter estimation and optimization software PEST by matching the M2 model results to observed aqueous concentrations of SO_4^{2-}, U, and Tc.

3. Results and discussion

3.1. Reaction path model M1

The geochemical processes governing changes in solution composition during titration were first simulated by an equilibrium reaction model that considered aqueous complexation and precipitation/dissolution reactions.

Precipitation of specific mineral phases computed by model M1 over the duration of the titration is shown in Fig. 1. Model M1 adequately described aqueous concentrations of Al, Fe (Fig. 2), and other metals, such as Ca, Mg, Mn, Ni and Co (not shown), but failed to accurately predict sulfate, U and Tc during titration (Fig. 2).

As pH increased during titration, decreasing aqueous concentrations were generally observed for Al, Fe (Fig. 2) and Co (not shown). Model M1 predicted that increasing pH first resulted in precipitation of Al, Fe, and Co hydroxide minerals, $Al_4SO_4(OH)_{10}$, $Al_2Si_2O_5(OH)_4$, and $FeCo_{0.1}(OH)_{3.2}$, because of their relatively low solubility (Fig. 1). The model predicted that most Al precipitated as $Al_4SO_4(OH)_{10}$ by pH ~ 5.0 and a majority of the Fe coprecipitated with Co forming $FeCo_{0.1}(OH)_{3.2}$ by pH ~ 5.5 (Fig. 1). When pH exceeded ~5, Al precipitated as $Al(OH)_3$ instead of $Al_4SO_4(OH)_{10}$ (Fig. 1). Therefore, in the early stages of the titration, solution pH should be largely buffered by the hydrolysis of Al and Fe resulting in the formation of aqueous hydrolysis species as well as solid phase hydroxides. Co precipitated as $Co(OH)_2$ when pH reached 8.5 in the NaOH titrated system. In the Na_2CO_3 titrated system, larger amounts of precipitate as $CoCO_3$ occurred above pH 6.5 due to higher dissolved carbonate concentrations in the latter system (Fig. 1).

Concentrations of Ca, Mg, Mn, and Ni remained relatively constant in the early stages of the titration but decreased with further increases in pH (not shown). Model M1 predicted that Mn precipitated as $MnCO_3$ when pH exceeded ~5.5; Ca coprecipitated with Mg forming $CaMg(CO_3)_2$ when pH exceeded ~6.0 and Ni precipitated as $Ni(OH)_2$ at pH above ~7.5 (Fig. 1). Therefore, in the late stage of the titration, solution pH should also be buffered by Ca, Mg, Mn, and Ni precipitates. Since more carbonate was introduced, more Ca, Mg, Mn, and Ni carbonate minerals were generated in the carbonate titrated system than in the hydroxide titrated system (Fig. 1).

When pH increased to ~4.5, a noticeable decrease in SO_4^{2-} concentration was observed (Fig. 2), suggesting coprecipitation or

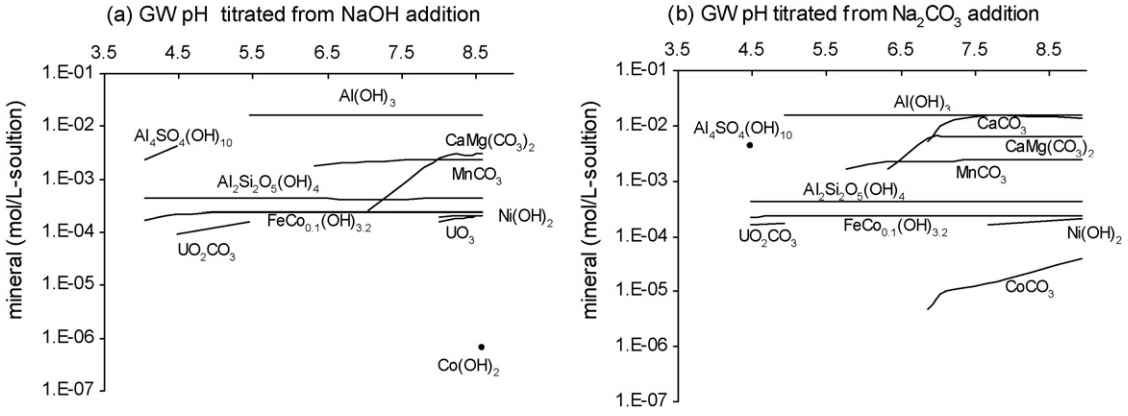

Fig. 1. Simulated mineral precipitation as a function of titrated pH.

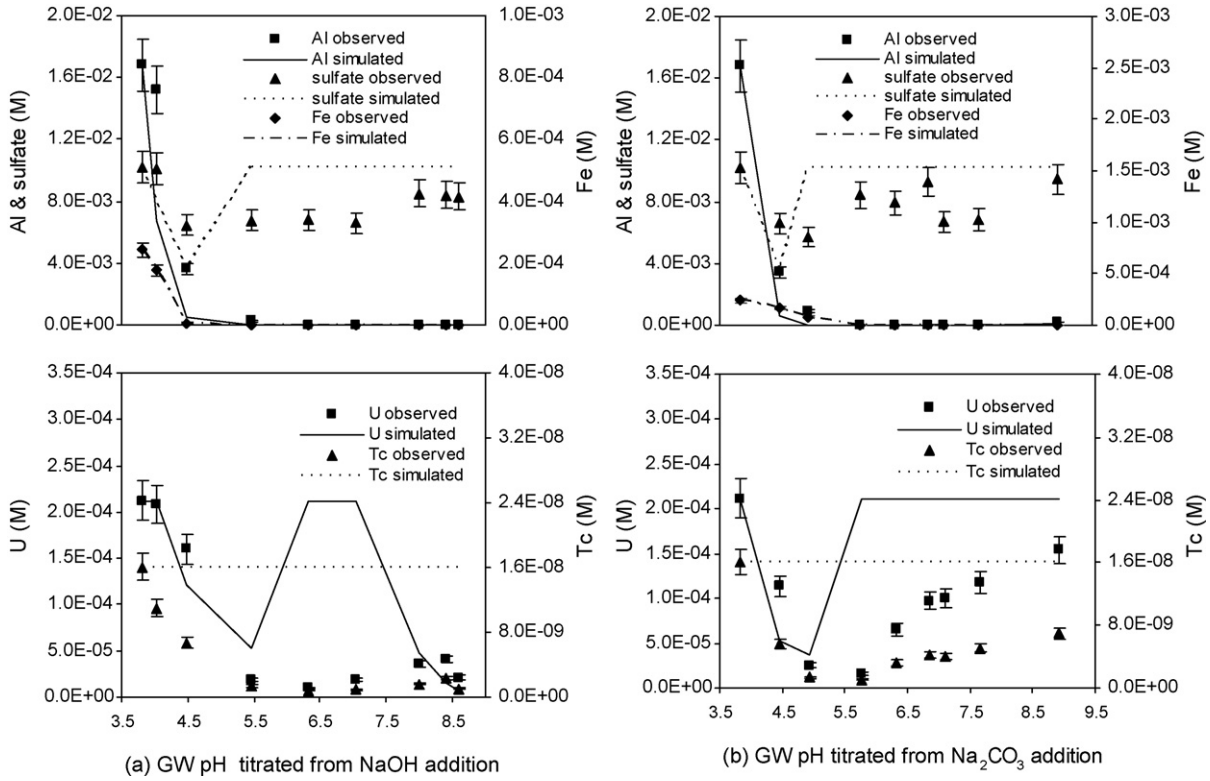

Fig. 2. Observed and M1 simulated aqueous concentrations of Al, sulfate, Fe, U and Tc as a function of titrated pH.

sorption of SO_4^{2-} to mixed solid phases. In the M1 model, loss of solution SO_4^{2-} was simulated by coprecipitation as a solid phase with a SO_4:Al:OH ratio of 1:4:10 and log K_{so} of 25 (Table 1). With further addition of NaOH, sulfate concentrations were predicted to increase as $Al_4(OH)_{10}SO_4$ altered to $Al(OH)_3$ (Fig. 1). Observed concentrations of SO_4^{2-} increased, but not to the extent seen in the M1 model prediction (Fig. 2).

Both U and Tc were rapidly removed from the solution above ~pH 5.5, which coincided with the precipitation of Al and Fe hydroxides. Concentrations of U and Tc increased with further increases in pH. Experimental results indicated that solution U and Tc decreased by more than 90% at pH ~ 5.5, while 70% of sorbed U and 40% of sorbed Tc returned to the aqueous phase as pH increased to ~9. In the M1 model, loss of solution phase U was simulated by precipitation as UO_2CO_3 at pH < 5.5 for both titrants and precipitation as UO_3 at pH > 7.5 for NaOH addition. At pH < 5.5, more UO_2CO_3 precipitated in the carbonate titrated system than in the hydroxide titrated system (Fig. 1), resulting in slightly quicker U removal from solution (Fig. 2). At pH > 7.5, no UO_3 precipitated in the carbonate titrated system (Fig. 1), resulting in higher U concentrations in solution (Fig. 2). The observed decrease of solution U was greater than predicted by the M1 model. Tc concentrations remained constant in the M1 model prediction as no precipitate of Tc was considered.

3.2. Reaction path model M2

The M2 model did a much better job describing sulfate, U and Tc concentrations than the M1 model (Fig. 3). As mentioned previously, a noticeable decrease in SO_4^{2-} concentration was observed in the early stages of the titration. In the M2 model, consumption of aqueous SO_4^{2-} was modeled by both coprecipitation of $Al_4(OH)_{10}SO_4$ (Table 1) and an ion exchange reaction representing sorption onto positively charged Al and Fe hydroxide surfaces (Table 2). With further addition of NaOH, the M2 model predicted increased sulfate concentrations as the positive surface charge of Al and Fe hydroxides diminished with increasing pH. As shown in Fig. 3, the simulated total concentrations of SO_4^{2-} using the M2 model are in good agreement with the observations. In the M1 model, loss of solution SO_4^{2-} was simulated by sulfate precipitation only. In the M2 model, loss of solution SO_4^{2-} occurred due to both sulfate precipitation and sorption. Consideration of sulfate sorption greatly improved the simulation accuracy (Figs. 2 and 3).

Previous studies have shown that all Fe and Al-oxyhydroxides strongly sorb dissolved U(VI) species [12,13]. It is therefore not surprising to observe rapid sorption or coprecipitation of U(VI) during titration at high dissolved Al concentrations due to precipitation of microcrystalline Al hydroxides. In the M2 model, consumption of aqueous uranium was modeled by both precipitation (e.g. $UO_2CO_{3(s)}$ in Table 1) and sorption onto positively charged Al and Fe hydroxide surfaces (Table 2).

As discussed above, speciation results of the M1 model led us to include anion exchange reactions for the $UO_2(CO_3)_2^{2-}$ and $UO_2(CO_3)_3^{4-}$ anions in the M2 model (Table 2). The M2 model predicted decreased AEC as the positive surface charge of Al and Fe hydroxides decreased with increasing pH. Observations of increased aqueous U(VI) with further pH increases may be attributed to the reduced sorption of uranyl-carbonate complexes by Al or Fe hydroxides due to reduced AEC at higher pH. Inclusion of uranium sorption significantly improved model predictions in the pH range of 5.5–8 for the NaOH titrated system and at pH > 5 for the Na_2CO_3 titrated system. In the M1 model, loss of solution U was simulated by uranium precipitation only. In the M2 model, loss of solution U was simulated by both uranium precipitation and sorption. Consideration of uranium sorption greatly improved simulation accuracy, especially for pH > 5.5 (Figs. 2 and 3).

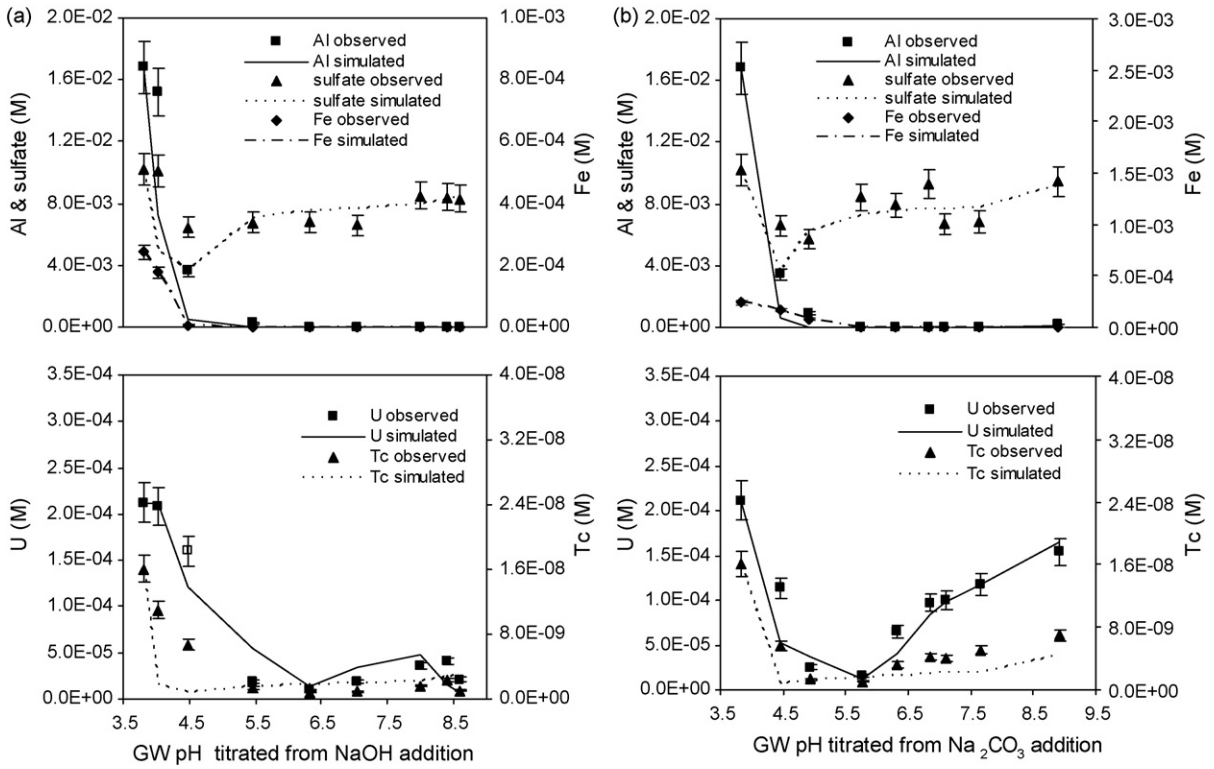

Fig. 3. Observed and M2 simulated aqueous concentrations of Al, sulfate, Fe, U and Tc as a function of titrated pH.

As shown in Fig. 3, removal of Tc coincided with precipitation of Al and Fe hydroxides. Unlike UO_2^{2+}, the anion TcO_4^- does not form carbonate species. Under the oxic conditions investigated, Tc hydroxide solids in reduced forms such as $TcO_2{\cdot}1.6H_2O$ are unlikely to occur in the system. Therefore, Tc removal is most likely attributable to electrostatic interactions between negatively-charged TcO_4^- and positively charged Fe and Al hydroxides, which exhibit zero points of charge (ZPC) in the range of 7.5–9.1 [30]. However, the fact that less desorption of Tc occurred at pH about 9 (Fig. 2) and the estimated parameters of sorption reactions (Table 2) suggest that Tc is more strongly sorbed than other anions such as sulfate, which was present in solution at 6 orders of magnitude higher concentration than Tc. These observations can be explained by the fact that TcO_4^- is a large, poorly hydrated anion and has a natural tendency to be strongly sorbed by a variety of adsorbents [8,10,18]. In the M1 model, no precipitation or sorption was considered for Tc, resulting in predictions of constant solution Tc concentration. In the M2 model, loss of solution U was simulated by sorption. Consideration of Tc sorption significantly improved simulation accuracy (Figs. 2 and 3).

The M2 model tracked gross features of U and Tc concentrations during titration, with deviations that we conjecture to be due to inaccurate representation of Al and Fe hydroxide precipitation. Carbonates may modify Al and Fe hydroxide surfaces in a manner that restricts U and TcO_4^- sorption [17,31]. Such effects were not considered in the model. Errors in predictions may also result from inaccurate estimates of solution phase carbonate because samples were neither purged nor equilibrated with atmospheric CO_2 ($P_{CO_2} = 10^{-3.5}$).

4. Conclusion

This study demonstrates the importance of sorption/desorption to mixed mineral phases on the acid–base behavior of radioactive U and Tc in groundwater containing multiple cationic and anionic species with a wide range of concentrations. Treating the complex mixture of Al and Fe minerals as an insoluble polyprotic base allows dynamic modeling of pH-dependent anion exchange capacity. Combining the ion exchange reactions with a geochemical reaction network describing hydrolysis and precipitation/dissolution has proven a practical and accurate means to simulate distributions of U and Tc between aqueous and solid phases during base addition. The proposed modeling approach could potentially provide an effective means to predict U and Tc mobility in response to pH manipulations performed in conjunction with groundwater remediation actions.

Dissolved carbonate was not measured during this study and the models assumed the titration system to be closed to the atmosphere [20]. For the NaOH titration, the titrant was assumed to contain 0.07 mol of total carbonate per mole NaOH [4,20]. In reality, CO_2 levels may vary over time and for each sample at various pH values. Since carbonate affects anionic uranyl-carbonate sorption, uncertainty in the amount of carbonate introduces some uncertainty in the estimation of U sorption parameters and indirectly induces uncertainty in the estimation of competing Tc sorption parameters. It is therefore suggested that future experiments include measurements of carbonates or be performed under controlled CO_2 conditions.

Acknowledgements

This research was funded by the U.S. Department of Energy, Office of Science, Biological and Environmental Research Programs. Oak Ridge National Laboratory is managed by UT-Battelle, LLC, for the U.S. Department of Energy under Contract DE-AC05-00OR22725.

Appendix A.

See Table A.1.

Table A.1
Aqueous complexation reactions considered in the model.

Aqueous complexation reaction	log *K*	References
$H_2O = H^+ + OH^-$	−14.0	[26]
$H_2CO_3^0 = H^+ + HCO_3^-$	−6.352	[26]
$HCO_3^- = H^+ + CO_3^{2-}$	−10.329	[26]
$H^+ + SO_4^{2-} = HSO_4^-$	1.988	[26]
$Na^+ + H_2O = NaOH^0 + H^+$	−14.18	[26]
$Na^+ + HCO_3^- = NaHCO_3^0$	−0.25	[26]
$Na^+ + CO_3^{2-} = NaCO_3^-$	1.27	[26]
$Na^+ + SO_4^{2-} = NaSO_4^-$	0.70	[26]
$K^+ + H_2O = KOH^0 + H^+$	−14.46	[26]
$K^+ + SO_4^{2-} = KSO_4^-$	0.85	[26]
$Ca^{2+} + H_2O = CaOH^+ + H^+$	−12.78	[26]
$Ca^{2+} + HCO_3^- = CaHCO_3^+$	1.106	[26]
$Ca^{2+} + CO_3^{2-} = CaCO_3^0$	3.224	[26]
$Ca^{2+} + SO_4^{2-} = CaSO_4^0$	2.30	[26]
$Mg^{2+} + H_2O = MgOH^+ + H^+$	−11.44	[26]
$Mg^{2+} + HCO_3^- = MgHCO_3^+$	1.07	[26]
$Mg^{2+} + CO_3^{2-} = MgCO_3^0$	2.98	[26]
$Mg^{2+} + SO_4^{2-} = MgSO_4^0$	2.37	[26]
$Sr^{2+} + H_2O = SrOH^+ + H^+$	−13.29	[26]
$Sr^{2+} + HCO_3^- = SrHCO_3^+$	1.18	[26]
$Sr^{2+} + CO_3^{2-} = SrCO_3^0$	2.81	[26]
$Sr^{2+} + SO_4^{2-} = SrSO_4^0$	2.29	[26]
$Mn^{2+} + H_2O = MnOH^+ + H^+$	−10.59	[26]
$Mn^{2+} + HCO_3^- = MnHCO_3^+$	1.95	[26]
$Mn^{2+} + CO_3^{2-} = MnCO_3^0$	4.90	[26]
$Mn^{2+} + SO_4^{2-} = MnSO_4^0$	2.25	[26]
$Mn^{2+} + Cl^- = MnCl^+$	0.61	[26]
$Mn^{2+} + 2Cl^- = MnCl_2^0$	0.25	[26]
$Mn^{2+} + 3Cl^- = MnCl_3^-$	−0.31	[26]
$Fe^{3+} + H_2O = FeOH^{2+} + H^+$	−2.19	[26]
$Fe^{3+} + 2H_2O = Fe(OH)_2^+ + 2H^+$	−5.67	[26]
$Fe^{3+} + 3H_2O = Fe(OH)_3^0 + 3H^+$	−12.56	[26]
$Fe^{3+} + 4H_2O = Fe(OH)_4^- + 4H^+$	−21.6	[26]
$2Fe^{3+} + 2H_2O = Fe_2(OH)_2^{4+} + 2H^+$	−2.95	[26]
$3Fe^{3+} + 4H_2O = Fe_3(OH)_4^{5+} + 4H^+$	−6.3	[26]
$Fe^{3+} + Cl^- = FeCl^{2+}$	1.48	[26]
$Fe^{3+} + 2Cl^- = FeCl_2^+$	2.13	[26]
$Fe^{3+} + 3Cl^- = FeCl_3^0$	1.13	[26]
$Fe^{3+} + SO_4^{2-} = FeSO_4^+$	4.04	[26]
$Fe^{3+} + 2SO_4^{2-} = Fe(SO_4)_2^-$	5.38	[26]
$Fe^{3+} + HSO_4^- = FeHSO_4^{2+}$	2.48	[26]
$Al^{3+} + H_2O = AlOH^{2+} + H^+$	−5.00	[26]
$Al^{3+} + 2H_2O = Al(OH)_2^+ + 2H^+$	−10.1	[26]
$Al^{3+} + 3H_2O = Al(OH)_3^0 + 3H^+$	−16.9	[26]
$Al^{3+} + 4H_2O = Al(OH)_4^- + 4H^+$	−22.7	[26]
$Al^{3+} + SO_4^{2-} = AlSO_4^+$	3.02	[26]
$Al^{3+} + 2SO_4^{2-} = Al(SO_4)_2^-$	4.92	[26]
$Al^{3+} + HSO_4^- = AlHSO_4^{2+}$	0.46	[26]
$Si(OH)_4^0 = SiO(OH)_3^- + H^+$	−9.83	[26]
$Si(OH)_4^0 = SiO_2(OH)_2^{2-} + 2H^+$	−23.0	[26]
$UO_2^{2+} + H_2O = UO_2OH^+ + H^+$	−5.25	[27]
$UO_2^{2+} + 2H_2O = UO_2(OH)_2^0 + 2H^+$	−12.15	[27]
$UO_2^{2+} + 3H_2O = UO_2(OH)_3^- + 3H^+$	−20.25	[27]
$UO_2^{2+} + 4H_2O = UO_2(OH)_4^{2-} + 4H^+$	−32.4	[27]
$2UO_2^{2+} + H_2O = (UO_2)_2OH^{3+} + H^+$	−2.7	[27]
$2UO_2^{2+} + 2H_2O = (UO_2)_2(OH)_2^{2+} + 2H^+$	−5.62	[27]
$3UO_2^{2+} + 4H_2O = (UO_2)_3(OH)_4^+ + 4H^+$	−11.9	[27]
$3UO_2^{2+} + 5H_2O = (UO_2)_3(OH)_5^+ + 5H^+$	−15.55	[27]
$3UO_2^{2+} + 7H_2O = (UO_2)_3(OH)_7^- + 7H^+$	−32.2	[27]
$4UO_2^{2+} + 7H_2O = (UO_2)_4(OH)_7^+ + 7H^+$	−21.9	[27]
$UO_2^{2+} + CO_3^{2-} = UO_2CO_3^0$	9.94	[27]
$UO_2^{2+} + 2CO_3^{2-} = UO_2(CO_3)_2^{2-}$	16.61	[27]
$UO_2^{2+} + 3CO_3^{2-} = UO_2(CO_3)_3^{4-}$	21.84	[27]
$UO_2^{2+} + 6CO_3^{2-} = UO_2(CO_3)_6^{6-}$	54.0	[27]
$2UO_2^{2+} + CO_3^{2-} + 3H_2O = (UO_2)_2CO_3(OH)_3^- + 3H^+$	−0.861	[27]
$3UO_2^{2+} + CO_3^{2-} + 3H_2O = (UO_2)_3O(OH)_2HCO_3^+ + 3H^+$	0.649	[27]
$11UO_2^{2+} + 6CO_3^{2-} + 12H_2O = (UO_2)_{11}(CO_3)_6(OH)_{12}^{2-} + 12H^+$	36.394	[27]
$UO_2^{2+} + NO_3^- = UO_2NO_3^+$	0.300	[27]
$UO_2^{2+} + SO_4^{2-} = UO_2SO_4^0$	3.15	[27]
$UO_2^{2+} + 2SO_4^{2-} = UO_2(SO_4)_2^{2-}$	4.14	[27]
$UO_2^{2+} + Cl^- = UO_2Cl^+$	0.17	[27]
$UO_2^{2+} + 2Cl^- = UO_2Cl_2^0$	−1.1	[27]

References

[1] A. Young, M. MacDonell, Facing the environmental risk issues of the cold war legacy, Environ. Sci. Pollut. Res. Int. 6 (1999) 186–187.
[2] R.G. Riley, J.M. Zachara, Chemical Contaminants on DOE Lands and Selection of Contaminant Mixtures for Subsurface Science Research, DOE/ER-0547T, 1992.
[3] B. Gu, D.B. Watson, D.H. Phillips, L. Liang, Biogeochemical, mineralogical, and hydrological characteristics of an iron reactive barrier used for treatment of uranium and nitrate, in: D.L. Naftz, et al. (Eds.), Groundwater Remediation of Trace Metals, Radionuclides, and Nutrients, With Permeable Reactive Barriers, Academic Press, 2002, pp. 305–342.
[4] F. Zhang, W. Luo, J.C. Parker, B.P. Spalding, S.C. Brooks, D.B. Watson, P.M. Jardine, B. Gu, Geochemical modeling of reactions and partitioning of trace metals and radionuclides during titration of contaminated acidic sediments, Environ. Sci. Technol. 42 (2008) 8007–8013.
[5] I. Grenthe, J. Fuger, R.J.M. Konings, R.J. Lemire, A.B. Muller, C.N.T. Cregu, H. Wanner, Chemical Thermodynamics of Uranium, North-Holland, 1992.
[6] M.C. Duff, C. Amrhein, Uranium(VI) adsorption on goethite and soil in carbonate solutions, Soil Sci. Soc. Am. J. 60 (1996) 1393–1397.
[7] J.A. Rard, in: M.C.A. Sandino, E. Osthols (Eds.), Chemical Thermodynamics of Technetium, North Holland/Elsevier, 1999.
[8] K. Schwochau, U. Pleger, Basic coordination chemistry of technetium, Radiochim. Acta 63 (1993) 103–110.
[9] B. Gu, G.M. Brown, P.V. Bonnesen, L. Liang, B.A. Moyer, R. Ober, S.D. Alexandratos, Development of novel bifunctional anion-exchange resins with improved selectivity for pertechnetate sorption from contaminated groundwater, Environ. Sci. Technol. 34 (2000) 1075–1080.
[10] E.H. Schulte, P. Scoppa, Sources and behavior of technetium in the environment, Sci. Total Environ. 64 (1987) 163–179.
[11] K.W. Paul, J.D. Kubicki, D.L. Sparks, Quantum chemical calculations of sulfate adsorption at the Al- and Fe-(Hydr)oxide–H_2O interface-estimation of Gibbs free energies, Environ. Sci. Technol. 40 (2006) 7717–7724.
[12] Z.Y. Tao, T.W. Chu, J.Z. Du, X.X. Dai, Y.J. Gu, Effect of fulvic acids on sorption of U(VI), Zn, Yb, I, and Se(IV) onto oxides of aluminum, iron, and silicon, Appl. Geochem. 15 (2000) 145–151.
[13] J.G. Catalano, T.P. Trainor, P.J. Eng, G.A. Waychunas, G.E. Brown, CTR diffraction and grazing-incidence EXAFS study of U(VI) adsorption onto α-Al_2O_3 and α-Fe_2O_3 (1 1 0 2) surfaces, Geochim. Cosmochim. Acta 69 (2005) 3555–3572.
[14] S. Kumar, N. Rawat, B.S. Tomar, V.K. Manchanda, S. Ramanathan, Effect of humic acid on the sorption of technetium on hematite colloids using Tc-95m and Tc-96 as tracers, J. Nucl. Radiochem. Sci. 274 (2007) 229–231.
[15] M.J. Kang, S.W. Rhee, H. Moon, V. Neck, T. Fanghanel, Sorption of MO_4^- (M = Tc, Re) on Mg/Al layered double hydroxide by anion exchange, Radiochim. Acta 75 (1996) 169–173.
[16] F. Zhang, S.C. Brooks, J.C. Parker, Y.-J. Kim, P.M. Jardine, D.B. Watson, Comparison of approaches to calibrate a surface complexation model for U(VI) sorption to weathered saprolite, Transp. Porous Media (2008), doi:10.1007/s11242-008-9294-9.
[17] T.D. Waite, J.A. Davis, T.E. Payne, G.A. Waychunas, N. Xu, Uranium(VI) adsorption to ferrihydrite: application of a surface complexation model, Geochim. Cosmochim. Acta 58 (1994) 5465–5478.
[18] R.E. Wildung, T.R. Garland, K.M. McFadden, C.E. Cowan, Technetium sorption in surface soils, Elsevier Appl. Sci. (1986).
[19] W. Luo, S.D. Kelly, K.M. Kemner, D. Watson, J. Zhou, P.M. Jardine, B. Gu, Sequestering uranium and technetium through co-precipitation with aluminum in a contaminated acidic environment, Environ. Sci. Technol. 43 (2009) 7516–7522.
[20] B. Gu, S.C. Brooks, Y. Roh, P.M. Jardine, Geochemical reactions and dynamics during titration of a contaminated groundwater with high uranium, aluminum, and calcium, Geochim. Cosmochim. Acta 67 (2003) 2749–2761.
[21] G.-T. Yeh, J.T. Sun, P.M. Jardine, W.D. Burgos, Y.L. Fang, M.H. Li, M.D. Siegel, HydroGeoChem 5.0: a three-dimensional model of coupled fluid flow, thermal transport, and hydrogeochemical transport through variable saturated conditions, Version 5.0, ORNL/TM-2004/107, 2004.
[22] F. Zhang, G.T. Yeh, J.C. Parker, S.C. Brooks, M.N. Pace, Y.-J. Kim, P.M. Jardine, D.B. Watson, A reaction-based paradigm to model reactive chemical transport in groundwater with general kinetic and equilibrium reactions, J. Contam. Hydrol. 92 (2007) 10–32.
[23] C.A.J. Appelo, D. Postma, Geochemistry, Groundwater and Pollution, 2nd ed., A.A. Balkema, 2005.
[24] J. Doherty (Ed.), PEST: Model Independent Parameter Estimation, Watermark Numerical Computing, 2004, p. 333.
[25] C.I. Steefel, S. Carroll, P. Zhao, S. Roberts, Cesium migration in Hanford sediment: a multisite cation exchange model based on laboratory transport experiments, J. Contam. Hydrol. 67 (2003) 219–246.
[26] W. Stumm, J.J. Morgan, Aquatic Chemistry, 3rd ed., John Wiley and Sons, 1996.
[27] R. Guillaumont, T. Fanghanel, V. Neck, J. Fuger, D.A. Palmer, I. Grenthe, M.H. Rand, Update on the Chemical Thermodynamics of Uranium, Neptunium, Plutonium, Americium, and Technetium, Elsevier, 2003.

[28] J.D. Prikryl, R.T. Pabalan, D.R. Turner, B.W. Leslie, Uranium sorption on alumina: effects of pH and surface-area/solution-volume ratio, Radiochim. Acta 66/67 (1994) 291–296.
[29] M.C. Arbestain, M.E. Barreal, F. Macias, Relating sulfate sorption in forest soils to lithological classes, as defined to calculate Critical Loads of Acidity, Sci. Total Environ. 241 (1999) 181–195.
[30] G. Sposito, The Surface Chemistry of Soils, Oxford University Press, 1984.
[31] J.D. Istok, In situ bioreduction of technetium and uranium in a nitrate contaminated aquifer, Environ. Sci. Technol. 38 (2004) 468–475.